A microRNA-24-to-secretagogin regulatory pathway mediates cholesterol-induced inhibition of insulin secretion

JING YANG[1*], YUNCHENG LV[2*], ZHIBO ZHAO[1], WU LI[1], SUNMIN XIANG[1], LINGZHI ZHOU[3], ANBO GAO[2], BIN YAN[1], LINGLING OU[1], HONG LING[4], XINHUA XIAO[1] and JIANGHUA LIU[1]

[1]Department of Endocrinology, The First Affiliated Hospital of The University of South China; [2]Laboratory of Clinical Anatomy and Reproductive Medicine, University of South China; Departments of [3]Paediatrics and [4]Emergency Surgery, The First Affiliated Hospital of The University of South China, Hengyang, Hunan 421001, P.R. China

Received October 3, 2018; Accepted May 20, 2019

DOI: 10.3892/ijmm.2019.4224

Abstract. Hypercholesterolemia is a key factor leading to β-cell dysfunction, but its underlying mechanisms remain unclear. Secretagogin (Scgn), a Ca^{2+} sensor protein that is expressed at high levels in the islets, has been shown to play a key role in regulating insulin secretion through effects on the soluble N-ethylmaleimide-sensitive factor attachment receptor protein complexes. However, further studies are required to determine whether Scgn plays a role in hypercholesterolemia-associated β-cell dysfunction. The present study investigated the involvement of a microRNA-24 (miR-24)-to-Scgn regulatory pathway in cholesterol-induced β-cell dysfunction. In the present study, MIN6 cells were treated with increasing concentrations of cholesterol and then, the cellular functions and changes in the miR-24-to-Scgn signal pathway were observed. Excessive uptake of cholesterol in MIN6 cells increased the expression of miR-24, resulting in a reduction in *Sp1* expression by directly targeting its 3' untranslated region. As a transcriptional activator of *Scgn*, downregulation of *Sp1* decreased Scgn levels and subsequently decreased the phosphorylation of focal adhesion kinase and paxillin, which is regulated by Scgn. Therefore, the focal adhesions in insulin granules were impaired and insulin exocytosis was reduced. The present study concluded that a miR-24-to-Scgn pathway participates in the mechanism regulating cholesterol accumulation-induced β-cell dysfunction.

Correspondence to: Dr Xinhua Xiao or Dr Jianghua Liu, Department of Endocrinology, The First Affiliated Hospital of The University of South China, 69 Chuanshan Road, Hengyang, Hunan 421001, P.R. China
E-mail: pingzhi9803@hotmail.com
E-mail: jianghua990@126.com

*Contributed equally

Abbreviations: GSIS, glucose-stimulated insulin secretion

Key words: miR-24, secretagogin, cholesterol, insulin secretion, β-cell

Introduction

Hyperlipidemia is a major contributing factor to the pathogenesis of β-cell dysfunction in subjects with type 2 diabetes (1). Hypercholesterolemia leads to the accumulation of cholesterol in islets and reduces insulin secretion, while a reduction in cholesterol levels restores insulin secretion. Excessive cholesterol accumulation in pancreatic β-cells not only affects the expression of insulin genes but also impairs the formation of insulin granules and their trafficking and fusion with the plasma membrane (2-5). However, the detailed mechanism by which high intracellular cholesterol levels affect insulin biosynthesis and secretion is not completely understood.

MicroRNAs (miRNAs/miR) are a class of short, nonprotein-coding gene products that target the 3' untranslated regions (3'UTRs) of mRNAs by repressing translation. Islet-specific miRNAs have been identified in mice and humans, and some of the dysregulated miRNAs are involved in the processes of insulin biosynthesis and exocytosis (6-9). miR-24 is a miRNA that is expressed at high levels in pancreatic β-cells and is shown to be further increased in islets from obese or high-fat diet-fed mice. Additionally, miR-24 regulates the expression of insulin gene transcriptional activators neuronal differentiation 1 (Neurod1) and Hnf1a, through which it negatively regulates insulin biosynthesis (10). Notably, miR-24 is the miRNA expressed at high levels in islets from db/db mice, leading to obesity, hyperglycemia, a reduction in insulin biosynthesis and an impairment in glucose-stimulated insulin secretion (GSIS) (10). However, the specific role of miR-24 in insulin secretion has not been explored.

Insulin secretion is a highly complex and concerted process that is orchestrated by a cascade of regulatory factors. Secretagogin (Scgn), an EF-hand Ca^{2+}-binding protein that is expressed at high levels in pancreatic β-cells, has been shown to be a positive regulator of insulin exocytosis through effects on actin dynamics and focal adhesion (11-13). Sp1, an experimentally verified transcriptional regulator of Scgn, which is involved in the control of GSIS (11), was predicted to harbor a putative miR-24 binding site in its 3'UTR. Therefore, it was speculated that cholesterol accumulation decreases insulin secretion in pancreatic β-cells and may be related to miR-24 overexpression. The present study also postulated that cholesterol-mediated

Sp1 downregulation inhibits the expression of Scgn and its downstream focal adhesion molecules, subsequently reducing the docking and fusion of insulin granules with the cell membrane. The present study sought to confirm the proposed molecular mechanisms of insulin secretion by employing MIN6 insulinoma cells as a model system.

Materials and methods

Cell culture. Mouse insulinoma-derived MIN6 cells (Fuheng Cell Center) were used for the functional and imaging experiments in the current study because of their stable response to glucose stimulation and low autofluorescence. Moreover, the MIN6 mouse β-cell line has been widely employed to assess the effect of cholesterol on pancreatic β-cells. The cells were maintained in Dulbecco's modified Eagle's medium (Gibco; Thermo Fisher Scientific, Inc.) containing 16.7 mM glucose and supplemented with 10% heat-inactivated fetal bovine serum (Gibco; Thermo Fisher Scientific, Inc.), 2 mM glutamine, 100 U/ml penicillin and 0.1 mg/ml streptomycin. The culture medium was changed every 3-4 days.

Oil red O staining. MIN6 cells were seeded in 6-well plates at a density of $1x10^6$ cells/well and grown overnight at 37˚C, and then incubated with water-soluble non-esterified cholesterol (Sigma-Aldrich; Merck KGaA) at 37˚C for 12 h. Then the cells were washed three times with PBS and fixed with 4% paraformaldehyde for 30 min at room temperature. A freshly diluted oil red O solution (Sigma-Aldrich; Merck KGaA) was added to each well and incubated for 15 min at room temperature, followed by decolorization with a 70% ethanol solution for 15 sec and staining with a hematoxylin solution for 30 sec at room temperature. After two rinses with distilled water, intracellular cholesterol droplets were observed and imaged under a fluorescence microscope at the light level (Leica Microsystems GmbH).

Determination of the intracellular cholesterol concentration. MIN6 cells were seeded in 12-well plates ($4x10^5$ cells/well), cultured overnight and subsequently treated with soluble cholesterol (Sigma-Aldrich; Merck KGaA). A total of 12 h after treatment, cells were harvested and the cholesterol content was quantified using a cholesterol assay kit (cat. no. MAK043; Sigma-Aldrich; Merck KGaA) according to the manufacturer's protocol. Briefly, $1x10^6$ cells were lysed in 200 μl of a mixture of chloroform: Isopropanol: NP-40 (7:11:0.1) with a microhomogenizer and then the supernatant was collected and dried in a vacuum. The dried lipids were dissolved in 200 μl of cholesterol assay buffer by sonication (at a frequency of 20 kHz with an on/off cycle of 10/10 sec repeated for 2 min at 4˚C) and vortexing until the solution appeared cloudy. Next, the reactions containing the cholesterol probe, esterase, enzyme mix, assay buffer and samples or standards were processed at 37˚C for 1 h. The absorbance was measured at 570 nm in a microplate reader and the intracellular cholesterol concentrations were adjusted for the DNA content.

Quantitation of the cell viability with the Cell Counting Kit-8 (CCK-8). MIN6 cells were cultivated in 96-well plates (5,000 cells/well) overnight and subsequently treated with different concentrations of cholesterol (0, 2.5, 5 or 10 mM) for 12 h. After removing the cell culture medium, 10 μl CCK-8 solution (Dojindo Molecular Technologies, Inc.) were added to each well of the plate and then incubated at 37˚C for 2 h. Finally, the absorbance was measured at 450 nm using a microplate reader.

miRNA transfection and mithramycin A (MMA) treatment. For the transfection assay, MIN6 cells were seeded in 24-well plates at a density of $2x10^5$ cells/well and grown overnight, followed by treatment with 5 mM cholesterol alone or in combination with 40 nM miR-24 mimic (cat. no. miR10000219-1-5; sequences commercially unavailable)/80 nM miR-24 inhibitor (cat. no. miR20000219-1-5; sequences commercially unavailable) for 48 h using the riboFECT™CP reagent according to the manufacturer's protocol (Guangzhou RiboBio Co., Ltd.). Meanwhile, a scrambled random miRNA sequence (5'-UUCUCCGAACGUGUCACGUTT-3'; 40 nM), which was commercially synthesized by Guangzhou RiboBio Co., Ltd., was used to treat the control cells. The expression level of miR-24 in these cells was identified at 48 h after transfection. In addition, MIN6 cells were pretreated with 10 μM MMA for 2 h and then subjected to the GSIS assay to identify the effect of direct inhibition of Sp1 expression on insulin secretion.

GSIS assay and determination of the insulin content. Insulin secretion and the insulin content in MIN6 cells were measured using an ELISA and normalized to the DNA content. Briefly, MIN6 cells were cultured in 24-well plates ($2x10^5$ cells/well) and grown overnight, and then incubated with cholesterol or in combination with the miR-24 mimic/miR-24 inhibitor for 48 h, the cells were subsequently incubated with KRB buffer supplemented with 3.3 mM glucose [5 mM KCl, 120 mM NaCl, 24 mM $NaHCO_3$, 15 mM Hepes (pH 7.4), 1 mM $MgCl_2$, 2 mM $CaCl_2$, 1 mg/ml ovalbumin] for 1 h. Next, cells were incubated with KRB buffer containing a stimulatory concentration of glucose (16.7 mM) for 30 min and the supernatant was collected to measure insulin concentration. After the GSIS assay, the cells were lysed in 200 μl of M-PER Mammalian Protein Extraction Buffer (Thermo Fisher Scientific, Inc.) and then centrifuged at 4,200 x g for 5 min at 4˚C, and the supernatants were harvested for the insulin content assay using a Mouse High Range Insulin ELISA kit (cat. no. 80-INSMSH-E01; ALPCO). The insulin concentrations were calculated and normalized to the DNA content, as determined using a Quant-iT™ dsDNA assay kit (Thermo Fisher Scientific, Inc.).

Immunofluorescence staining. Immediately after the GSIS assay, the insulin content in MIN6 cells ($2x10^5$ cells/well) was also detected using immunofluorescence staining. Briefly, cells were fixed with a freshly prepared solution of 4% paraformaldehyde for 20 min at room temperature, followed by permeabilization with 0.1% Triton X-100 for 10 min. After blocking with PBS-Tween-3% bovine serum albumin (Sigma-Aldrich; Merck KGaA) for 1 h, cells were incubated with a primary antibody against insulin (cat. no. I2018; 1:200; Sigma-Aldrich; Merck KGaA) overnight at 4˚C and then incubated with a fluorescein isothiocyanate-conjugated secondary antibody (cat. no. 711-545-1500; 1:200; Jackson ImmunoResearch Laboratories, Inc.) for 1 h, followed by nuclear staining with DAPI. Images of the immunofluorescence

Table I. Primers sequences used for *miR-24*, *Ins1*, *Ins2* and *Scgn* amplification.

Gene	Forward primer (5'-3')	Reverse primer (5'-3')
miR-24	TGGCTCAGTTCAGCAGGAACAG	Unique quantitative-PCR reverse primer from the cDNA Synthesis kit
Ins1	CTTGCCCTCTGGGAGCCCA	TGAAGGTCCCCGGGGCTTC
Ins2	CCACAAGTGGCACAACTGGA	CTACAATGCCACGCTTCTGC
Scgn	CCCAGAAGTGGATGGATTTG	GTTGGGGATCAGGGGTTTAT

SCGN, secretagogin; miR, microRNA.

staining were captured with a fluorescence microscope (Carl Zeiss AG).

Reverse transcription-quantitative PCR (RT-qPCR) analysis. Total RNA was extracted using the TRIzol reagent (Thermo Fisher Scientific, Inc.) and reverse transcribed with MMLV Reverse Transcription Reagents at 37˚C for 1 h (Promega Corporation). Relative qPCR was performed using SYBR-Green detection chemistry (Qiagen, Inc.) on a PRISM 7500HT Real-Time PCR System (Applied Biosystems; Thermo Fisher Scientific, Inc.). The thermocycling reaction consisted of the following conditions: 1 cycle at 95˚C for 15 min, followed by 40 cycles of a denaturation step at 95˚C for 15 sec, an annealing step at 60˚C for 30 sec, and an extension step at 70˚C for 30 sec. The expression levels of miR-24, *Ins1*, *Ins2* and *Scgn* were validated using RT-qPCR. The U6 small nuclear RNA and *Gapdh* were used as endogenous controls for miRNA and mRNAs, respectively, and the relative gene expression data were analyzed using the $2^{-\Delta\Delta Cq}$ method (14). The primers used for RT-qPCR are described in Table I.

Bioinformatics analysis and luciferase reporter assays. The miR-24 sequences were obtained from miRBase database and its target genes were predicted using online websites, TargetScan and miRanda. The minimum free energy of the hybridization between Sp1 3'UTR and miR-24 was analyzed with RNAhybrid. A total of transcription factor prediction databases, PROMO, Tfsitescan and DBD, were used to predict whether there is a direct interaction between Sp1 and the *Ins1* promoter. The detailed websites of these databases are listed in the supplementary file: Table SI.

The 3'UTR of *Sp1*, which was predicted to contain the putative target site for miR-24, was amplified by RT-PCR from total RNA extracted from MIN6 cells with primers containing *Xho*I and *Not*I sites. For comparison, site-directed mutagenesis was used to introduce the seed region of the predicted miR-24 binding sites within the 3'UTR of *Sp1* using a Multisite-Quick Change kit (Agilent Technologies, Inc.). Wild-type and mutant inserts were cloned into a psiCHECK™-2 vector (Promega Corporation). Each recombinant plasmid was confirmed by sequencing (Takara Biotechnology Co., Ltd.) and then cotransfected with a miR-24 mimic into 293T cells (Fuheng Cell Center). Luciferase activity was measured using the Dual-Glo Luciferase Assay System (Promega Corporation) at 48 h post-transfection. The relative luciferase activity of each group was reported as the percentage of *Renilla* luciferase activity normalized to the corresponding firefly luciferase activity.

Western blotting analysis. At 30 min after stimulation with high glucose (16.7 mM), MIN6 cells were washed twice with PBS and cellular proteins were extracted with M-PER Mammalian Protein Extraction Buffer (Thermo Fisher Scientific, Inc.). Protein concentration was measured using a BCA protein quantitation kit (Beyotime Institute of Biotechnology). Total cellular proteins (30 μg) were fractionated on 10% SDS-PAGE gels. Proteins were transferred to PVDF membranes and then western blotting was performed according to standard procedures described in a previous study (15). The primary antibodies used were as follows: Anti-Scgn antibody (cat. no. ab137017; 1:2,000; Abcam), anti-Sp1 antibody (cat. no. ab227383; 1:1,000), anti-focal adhesion kinase (FAK) antibody (cat. no. 3285; 1:1,000; Cell Signaling Technology, Inc.), anti-phospho-FAK (Tyr^{397}) antibody (cat. no. 3283; 1:1,000; Cell Signaling Technology, Inc.), anti-paxillin antibody (cat. no. 2542; 1:1,000; Cell Signaling Technology, Inc.), anti-phospho-paxillin (Tyr^{118}) antibody (cat. no. 2541; 1:1,000; Cell Signaling Technology, Inc.) and β-actin antibody (cat. no. 3700; 1:2,000; Cell Signaling Technology, Inc.). Accordingly, a horseradish peroxidase-conjugated goat anti-rabbit immunoglobulin G secondary antibody (cat. no. A0208; 1:2,000; Beyotime Institute of Biotechnology) and goat anti-mouse antibody (cat. no. A0216; 1:2,000; Beyotime Institute of Biotechnology) were used to detect the proteins.

Statistical analysis. All data are presented as the mean ± standard deviation and significant differences were assessed using one-way ANOVA followed by Student-Newman-Keuls test. SPSS statistical software (version 18.0; IBM Corp.) was used to conduct the data analysis. $P<0.05$ was considered to indicate a statistically significant difference. Independent experiments were performed at least three times.

Results

Accumulation of cholesterol in MIN6 cells induces miR-24 expression. A total of 4 groups of cells treated with increasing concentrations of cholesterol (0, 2.5, 5.0 or 10.0 mM for 12 h) were evaluated using RT-qPCR to determine the changes in miR-24 expression in cholesterol-treated MIN6 cells. Cholesterol induced a dose-dependent increase in the intracellular cholesterol content in MIN6 cells (Fig. 1A and B). Meanwhile, miR-24 expression was significantly increased as the cholesterol concentration increased from 0-5 mM ($P<0.01$) and an increase,

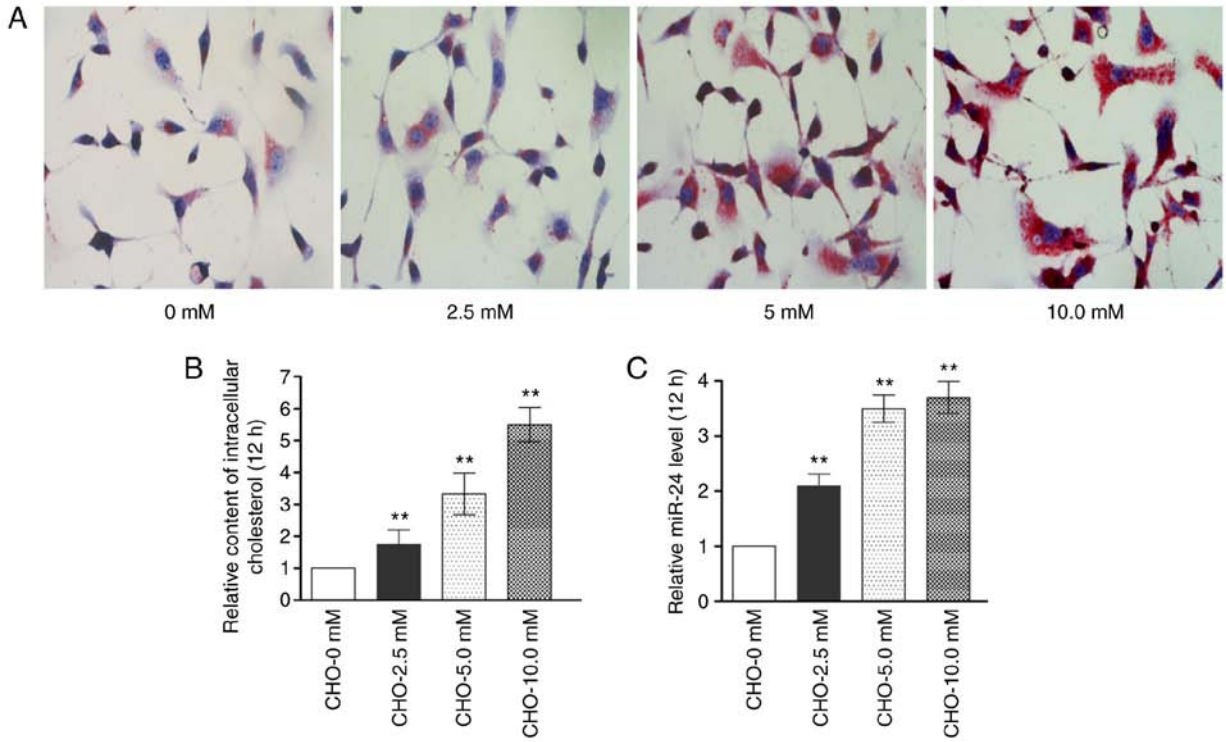

Figure 1. Changes in lipid accumulation and miR-24 expression in CHO-treated MIN6 cells. (A) MIN6 cells were treated with 0, 2.5, 5.0 or 10.0 mM cholesterol for 12 h and the intracellular cholesterol was observed using oil red O staining (original magnification, x400). (B) The intracellular cholesterol content was analyzed using a cholesterol assay kit, as described in the methods. (C) Expression of miR-24 in MIN6 cells treated with increasing concentrations of CHO. **P<0.01 vs. the 0 mM CHO-treated group. CHO, cholesterol; miR, microRNA.

although to a lesser extent, was observed as the cholesterol concentration further increased from 5-10 mM (Fig. 1C). Since this study focuses on insulin biosynthesis and secretion in β-cells, a 5 mM soluble cholesterol concentration which is greater than the concentration in normal culture medium was demonstrated to have little impact on cell viability (Fig. S1A); therefore, this concentration was used in the subsequent experiments.

Cholesterol accumulation in MIN6 cells inhibits Ins1 expression and insulin secretion. The effects of cholesterol accumulation in MIN6 cells on insulin mRNA expression and insulin secretion were determined by exposing cells to 5 mM cholesterol for 12 h. Based on the results of the RT-qPCR assays, the expression of the *Ins1* mRNA was significantly reduced in MIN6 cells treated with cholesterol alone or in combination with 40 nM miR-24 mimic (P<0.01), whereas the expression of *Ins2* was not decreased (Fig. 2A). Meanwhile, GSIS was significantly reduced in cells treated with cholesterol alone or in combination with the miR-24 mimic (P<0.01; Fig. 2B). In general, the intracellular insulin content increased by ~50% in β-cells treated with cholesterol alone or in combination with the miR-24 mimic, indicating that cholesterol alone or in combination with the miR-24 mimic inhibited insulin secretion to a greater extent than insulin transcription. Notably, the miR-24 inhibitor rescued the reductions in insulin transcription and secretion, particularly insulin secretion, induced by the treatment with cholesterol alone or in combination with the miR-24 mimic, which subsequently decreased the insulin content in MIN6 cells (Fig. 2C-D). Therefore, the cholesterol-induced decrease in insulin secretion is associated with increased miR-24 expression.

Cholesterol inhibits the expression of Scgn at both the mRNA and protein levels. The expression of *Scgn* was evaluated in MIN6 cells treated with cholesterol alone or in combination with a miR-24 mimic/miR-24 inhibitor to investigate the mechanism underlying the effect of cholesterol on insulin secretion. After confirming the successful modulation of miR-24 expression (Fig. S1B), cholesterol alone or in combination with a miR-24 mimic significantly reduced in Scgn expression at both the mRNA and protein levels (P<0.01), whereas the reduction was markedly rescued after co-incubation with a miR-24 inhibitor for 12 h (Fig. 3). These results indicate a regulatory relationship between miR-24 and Scgn.

Sp1 is a direct target gene of miR-24. Notably, miR-24 is broadly conserved among diverse species, indicating that it has biological functions under physiological and/or pathological conditions (Fig. 4A). Although miR-24 expression was significantly increased in cholesterol-treated MIN6 cells, its function in insulin secretion is largely unknown. Potential target genes of miR-24 were first searched for using the online analysis programs mentioned in the methods to further investigate the regulatory relationship between miR-24 and *Scgn*, but putative miR-24 binding sites within the 3'UTR of the *Scgn* mRNA were not identified. However, Sp1, an experimentally confirmed transcriptional activator of the *Scgn* gene (11), contains a putative miR-24 binding site within its 3'UTR. Interestingly, low free energy scores (in RNAhybrid) for the hybridization of miR-24 and the *Sp1* mRNA were observed in mice and humans, suggesting that miR-24 most likely directly targets the 3'UTR of the *Sp1* mRNA and represses its

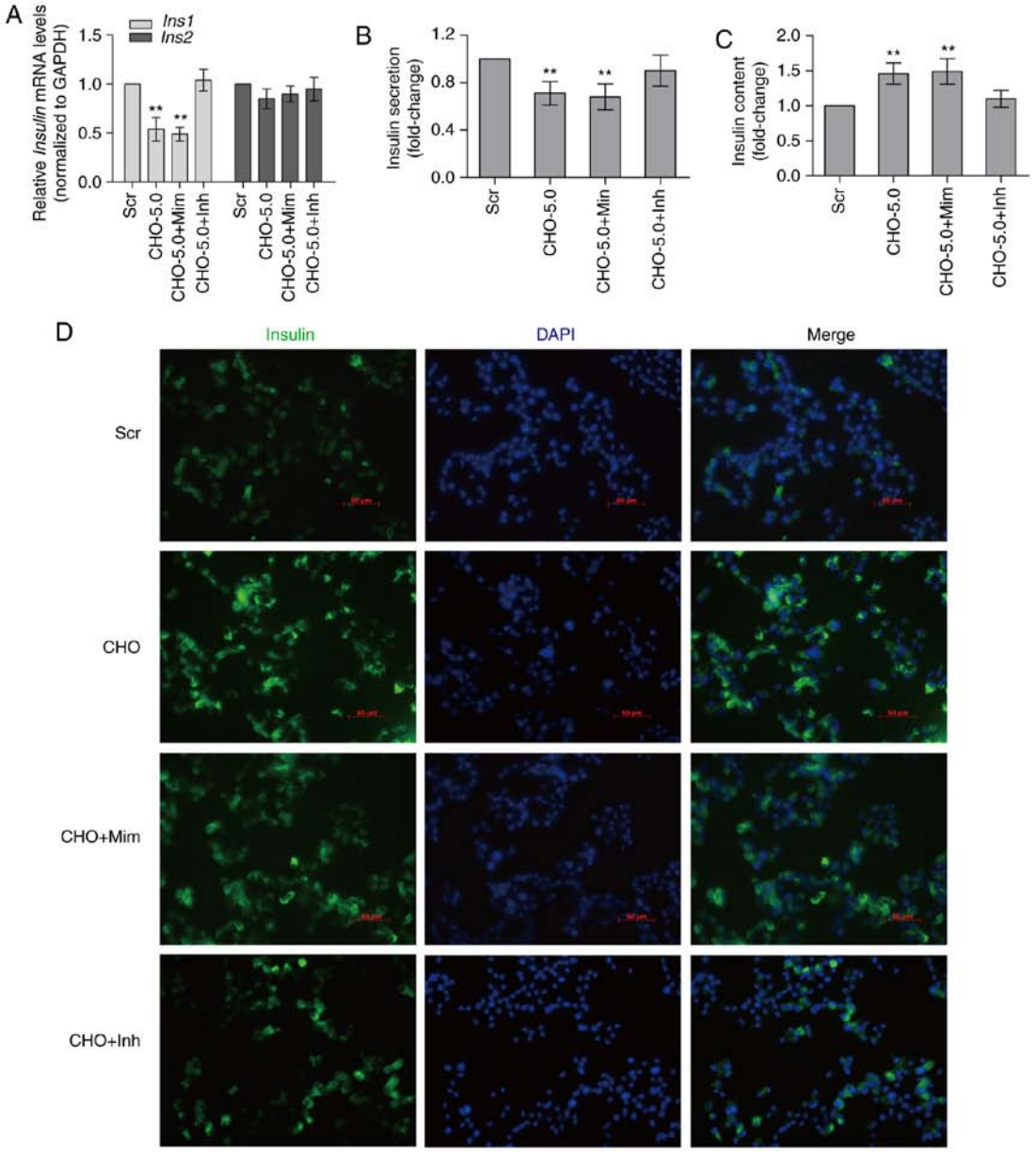

Figure 2. miR-24 is involved in the CHO-mediated inhibition of insulin secretion in MIN6 cells. (A) Treatment with 5.0 mM CHO alone or in combination with miR-24 mimic significantly decreased the expression of *Ins1* mRNA and the decrease was rescued by the miR-24 inhibitor, whereas the expression of the *Ins2* mRNA was not altered. (B) Treatment with CHO alone or in combination with the miR-24 mimic for 12 h decreased glucose-stimulated insulin secretion in MIN6 cells, while the miR-24 inhibitor rescued the reduction in insulin secretion. The insulin content in MIN6 cells was analyzed using (C) an ELISA and (D) immunofluorescence staining 12 h after treatment (scale bars, 50 μm). **P<0.01 vs. the Scr-treated group. Scr, scrambled miRNA sequence; CHO, cholesterol; Mim, miR-24 mimic; Inh, miR-24 inhibitor; miR, microRNA.

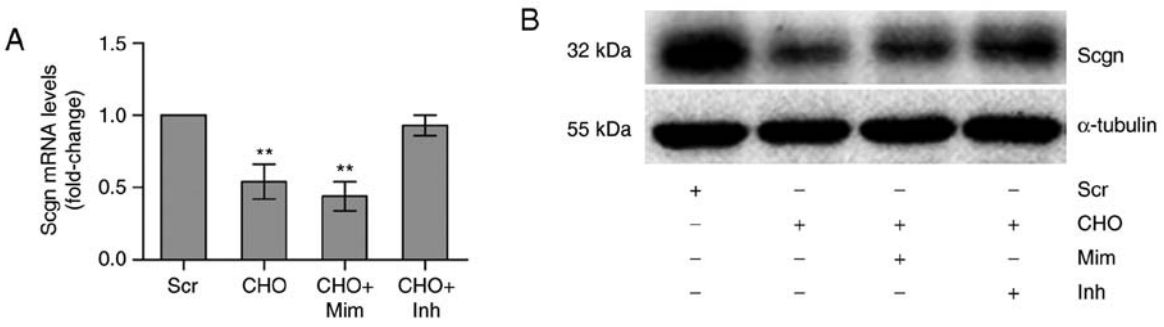

Figure 3. Effect of the CHO treatment on the levels of the Scgn mRNA and protein in MIN6 cells. Levels of the Scgn (A) mRNA and (B) protein were measured using reverse transcription quantitative PCR or western blotting, respectively, in MIN6 cells treated with 5.0 mM CHO alone or in combination with 40 nM miR-24 mimic/80 nM miR-24 inhibitor for 12 h. **P<0.01 vs. the Scr-treated group. Scr, scrambled miRNA sequence; CHO, cholesterol; Mim, miR-24 mimic; Inh, miR-24 inhibitor; Scgn, secretagogin.

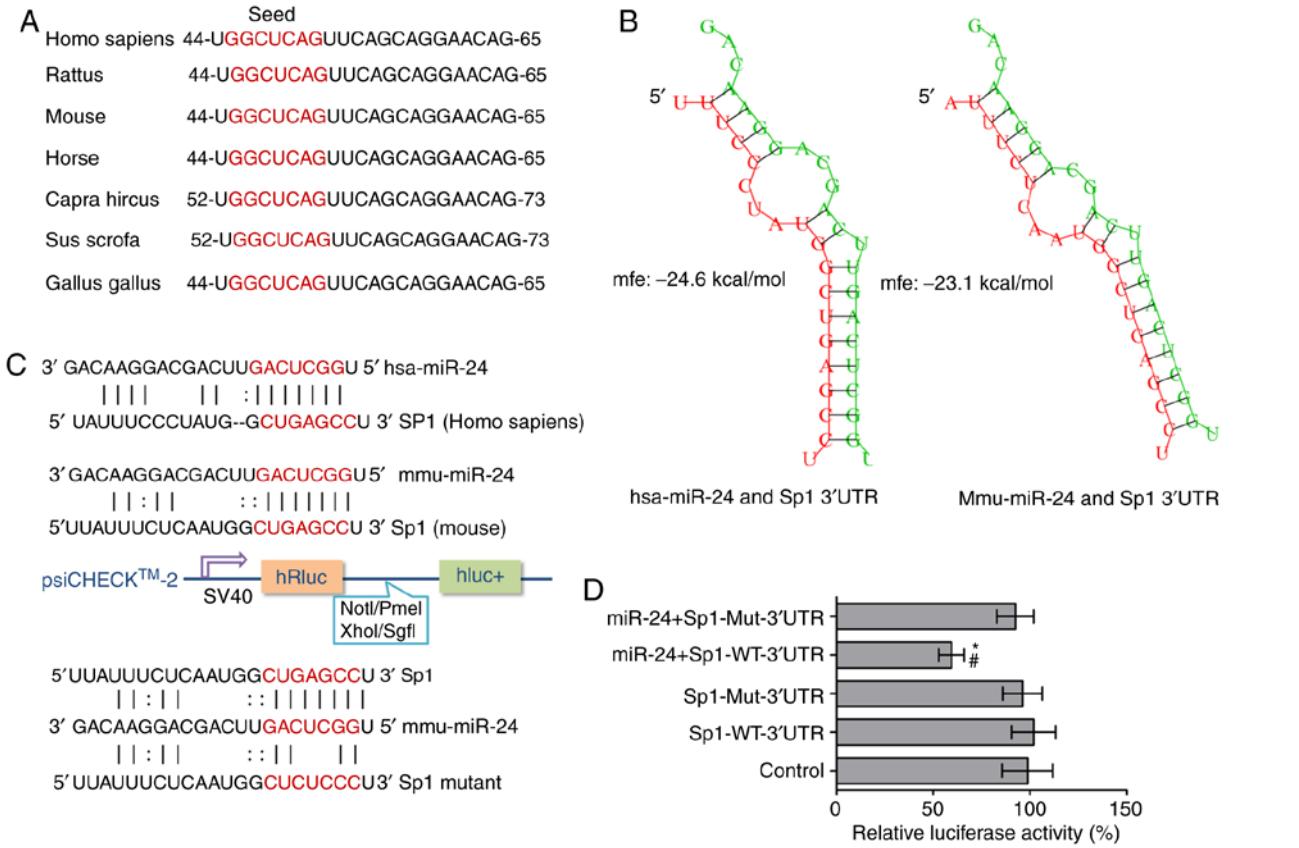

Figure 4. Bioinformatics prediction and experimental verification that miR-24 directly targets the *Sp1* 3'UTR. (A) The highly evolutionary conserved miR-24 targeting sequences from different species. (B) The free energy scores (in RNAhybrid) for miR-24 hybridization to the human and mouse *Sp1* sequence. (C) The putative miR-24 binding sites within the human and mouse *Sp1* 3'UTR and the mutant sequences in the luciferase reporter plasmid are shown. (D) Luciferase activity assays in 293T cells cotransfected with the control luciferase reporter plasmid and a recombinant plasmid containing the WT or Mut *Sp1* 3'UTR and miR-24 mimic for 24 h. *P<0.05 vs. the control; #P<0.05 vs. the Sp1-WT 3'UTR group. UTR, untranslated region; WT, wild type; Mut, mutant; miR, microRNA.

expression (Fig. 4B). Furthermore, *in silico* promoter analysis excluded a potential direct interaction between Sp1 and the *Ins1* promoter (data not shown).

Next, a luciferase reporter assay was performed in 293T cells to verify the direct targeting effect of miR-24 on the 3'UTR of the *Sp1* mRNA. psi-CHECK™-2 luciferase vectors were constructed harboring the wild-type (Sp1-WT) or mutant (Sp1-Mut) sequence of the mouse *Sp1* 3'UTR, in which the putative miR-24 binding site 5'-CUGAGCC-3' was mutated to 5'-CUCUCCC-3' (Fig. 4C). Meanwhile, a vector containing a nonrelated cDNA fragment was constructed as a control. Following the cotransfection of the miR-24 mimic with Sp1-WT, Sp1-Mut or a control, the luciferase activity in the Sp1-WT transfected cells was significantly reduced by the miR-24 mimic (P<0.05), whereas it was not affected in the Sp1-Mut and control groups (Fig. 4D). Based on these results, miR-24 plays a crucial role in the posttranscriptional repression of *Sp1* expression via directly targeting its 3'UTR.

miR-24 regulates the Scgn/FAK/paxillin pathway in cholesterol-treated MIN6 cell by targeting Sp1. The miR-24 mimic or miR-24 inhibitor was transfected into cholesterol-treated MIN6 cells and the levels of Sp1, Scgn, FAK, phosphorylated (p)-FAK, Paxillin and p-paxillin were measured using western blotting to confirm whether miR-24 inhibited insulin secretion by directly regulating Sp1 expression and the GSIS pathway. Cholesterol-induced overexpression of miR-24 decreased the levels of Sp1, Scgn and its downstream focal adhesion molecules, p-FAK and p-paxillin, during GSIS. In contrast, the miR-24 inhibitor significantly rescued the reduction in Sp1, Scgn, p-FAK and p-paxillin levels during the GSIS process (P<0.01; Figs. 3B and 5).

In parallel, an experiment designed to identify the effect of direct inhibition of Sp1 function on insulin secretion in MIN6 cells was conducted. The inhibition of Sp1 function by a pretreatment with the Sp1 inhibitor MMA (10 mM for 2 h) decreased the levels of the Scgn, p-FAK and p-paxillin proteins and attenuated GSIS (Fig. S2). Furthermore, online analysis of the *Ins1* promoter sequence did not identify a Sp1-binding site, which excludes a direct interaction between the Sp1 protein and this mRNA. Therefore, cholesterol-induced overexpression of miR-24 inhibits GSIS by negatively regulating *Sp1* expression and the Scgn/FAK/paxillin pathway.

Discussion

Type 2 diabetes is often associated with hypercholesterolemia. Previous evidence has shown that excessive accumulation of palmitate in β-cells could lead to β-cell dysfunction and

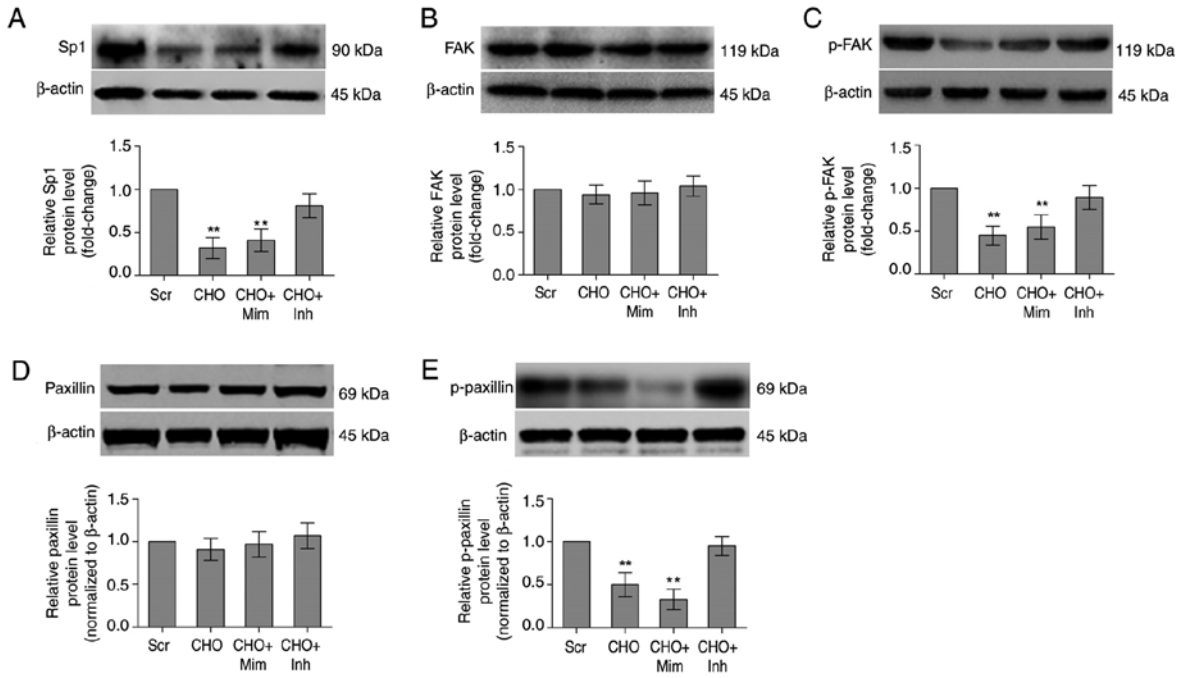

Figure 5. CHO affects the levels of proteins involved in the Sp1/Scgn-FAK signaling pathway mediating insulin trafficking. Changes in the levels of the Sp1, FAK, p-FAK, paxillin and p-paxillin proteins in MIN6 cells treated with 5.0 mM CHO alone or in combination with 40 nM miR-24 mimic/80 nM miR-24 inhibitor for 12 h were measured using western blotting assay. β-Actin served as the loading control. (A) Sp1, (B) FAK, (C) p-FAK (D) paxillin and (E) p-paxillin. **P<0.01 vs. the Scr-treated group. Scr, scrambled miRNA sequence; CHO, cholesterol; Mim, miR-24 mimic; Inh, miR-24 inhibitor; Scgn, secretagogin; p-FAK, phosphorylated-focal adhesion kinase; miR, microRNA.

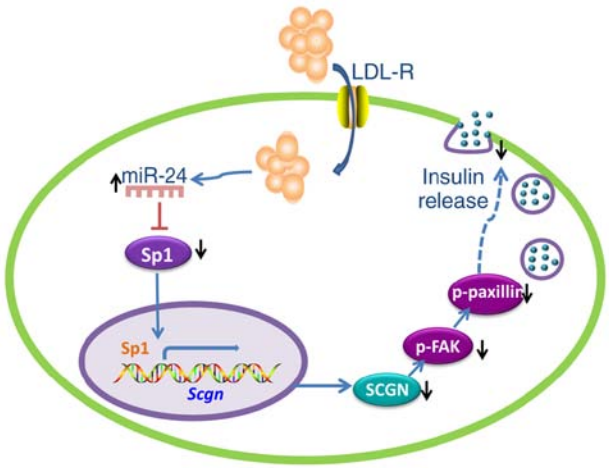

Figure 6. Schematic summarizing the potential pathogenic mechanism underlying CHO-mediated inhibition of insulin secretion. Intracellular CHO accumulation induces miR-24 expression in MIN6 cells and then decreases the expression of *Sp1*. The levels of Scgn and its downstream insulin granule trafficking-related proteins are decreased and insulin secretion is subsequently decreased. CHO, cholesterol; ↑, induction; ↓, inhibition. SCGN, secretagogin; p-FAK, phosphorylated-focal adhesion kinase; miR, microRNA; LDL-R, low-density lipoprotein receptor.

the development of diabetes (10,16,17). In addition to the uptake of palmitate, β-cells also take up cholesterol through their high-affinity low density lipid receptors (5). Cholesterol accumulation in the islets may contribute to insulin-producing β-cell dysfunction and the loss of GSIS. However, a role for hypercholesterolemia in the pathogenesis of type 2 diabetes is not well established. In the present study, a novel molecular mechanism was investigated by which cholesterol inhibits insulin secretion in MIN6 cells. As shown in Fig. 6, cholesterol accumulation in MIN6 cells increased the expression of miR-24 and miR-24 overexpression silenced the expression of *Sp1* by directly targeting its 3'UTR. As a transcriptional activator of *Scgn*, downregulation of *Sp1* resulted in a concomitant reduction in Scgn expression, followed by a decrease in the levels of the downstream proteins p-FAK and p-paxillin, which regulate the focal adhesion process in insulin granules. GSIS was subsequently impaired.

As shown in recent studies, miRNAs are key factors involved in the mechanisms regulating insulin biosynthesis, the trafficking of granules and insulin secretion (18-20). The highest expression of miR-24 was observed in islets isolated from genetically obese or high-fat diet-fed mice, as well as in islets treated with palmitate (10). In the study by Zhu *et al* (10), miR-24 repressed the insulin biosynthesis process by targeting two maturity onset diabetes of the young genes, *Hnf1a* and *Neurod1*, leading to reductions in both basal and stimulated-insulin secretion. In addition to affecting insulin biosynthesis, further studies are needed to determine whether miR-24 also regulates the insulin secretion process. In the present study, dose-dependent cholesterol accumulation concomitant with miR-24 upregulation in cholesterol-treated MIN6 cells was revealed. Intriguingly, following the increase in miR-24 expression, *Ins1* mRNA expression was reduced, whereas the *Ins2* mRNA was unaffected. These results are consistent with existing evidence that *Ins1* expression is significantly decreased and *Ins2* expression is not affected in *NeuroD* conditional knockout mice (21), suggesting that cholesterol-induced miR-24 upregulation in MIN6 may repress *Ins1* expression by targeting *NeuroD*. The level of *Ins2* mRNA is 9-fold higher than the *Ins1* mRNA in MIN6

cells (22), therefore, miR-24-mediated *Ins1* mRNA silencing may have a limited effect on insulin protein biosynthesis.

Since a significant decrease in insulin secretion and a marked increase in the insulin content were observed in cholesterol-treated MIN6 cells after GSIS, changes in the expression of Scgn, a key regulator of insulin secretion that was recently identified were subsequently detected (12,13,23,24) and observed a dramatic decrease in response to the cholesterol treatment. A bioinformatics analysis was next conducted to predict interactions between miR-24 and *Scgn*. Although a direct interaction between miR-24 and *Scgn* was not identified, a putative miR-24 binding site within the *Sp1* 3'UTR was predicted and experimentally identified. Following the downregulation of *Sp1*, the expression of *Scgn,* which is transcriptionally regulated by Sp1 (11), was subsequently downregulated. It was excluded a potential direct interaction between Sp1 and the *Ins1* promoter, which further supports that miR-24 decreases insulin secretion rather than insulin biosynthesis through Sp1.

Scgn is specifically expressed in pancreatic islets at high levels and further elevated in islets and plasma from patients and rats with type 2 diabetes mellitus (12,25-27). Scgn is a pivotal regulator of insulin secretion that functions by activating focal adhesion complexes, including FAK, paxillin and F-actin, and modulating the focal adhesion process (13,28). Silencing of focal adhesion complexes impairs the docking and release of insulin granules (29,30). Consistent with the results of these studies, the present study observed decreased levels of p-FAK and paxillin following the downregulation of Scgn. Notably, the suppression of the Sp1/Scgn/FAK signaling pathway was rescued by a miR-24 inhibitor, which further confirmed that a miR-24-to-Scgn regulatory pathway mediates cholesterol-induced inhibition of insulin secretion.

Collectively, cholesterol accumulation in MIN6 pancreatic β-cells increases miR-24 expression and miR-24 is a negative regulator of Sp1. The miR-24-to-Scgn regulatory pathway was proven to regulate focal adhesion, a critical step in insulin secretion, in cholesterol-treated MIN6 cells. Moreover, miR-24 inhibition is probably a therapeutic strategy for cholesterol-induced β-cell dysfunction by regulating Scgn-mediated insulin secretion. However, understanding of the relationship between hypercholesterolemia and the miR-24-to-Scgn regulatory pathway is still at an early stage. Further investigations are warranted to illuminate how cholesterol accumulation increases the expression of miR-24 in β-cells and whether miR-24 manipulates insulin secretion by targeting other genes. Further studies designed to establish whether the miR-24-to-Scgn pathway is impaired during insulin exocytosis in patients with hypercholesterolemia *in vivo* are needed.

Acknowledgements

Not applicable.

Funding

The present study was financially support by The National Natural Sciences Foundation of China (grant no. 81770460), The Aid Program (grant no. 2017KJ268), The Construction Program of Innovation Platform (grant no. 2017KJ182) from Science and Technology Bureau of Hengyang City, and The Third Level of Chuanshan Talent Project of University of South China (grant no. 2017CST20).

Availability of data and materials

All data generated or analyzed during this study are included in this published article.

Authors' contributions

XHX and JHL designed the experiments. JY, YCL, ZBZ, WL, SMX, LZZ, LLO and ABG performed the experiments. BY and HL analyzed the data. JY and LLO wrote and revised the manuscript. All authors read and approved the final manuscript.

Ethics approval and consent to participate

Not applicable.

Patient consent for publication

Not applicable.

Competing interests

The authors declare that they have no competing interests.

References

1. Brunham LR, Kruit JK, Verchere CB and Hayden MR: Cholesterol in islet dysfunction and type 2 diabetes. J Clin Invest 118: 403-408, 2008.
2. Hao M, Head WS, Gunawardana SC, Hasty AH and Piston DW: Direct effect of cholesterol on insulin secretion: A novel mechanism for pancreatic beta-cell dysfunction. Diabetes 56: 2328-2338, 2007.
3. Xu Y, Toomre DK, Bogan JS and Hao M: Excess cholesterol inhibits glucose-stimulated fusion pore dynamics in insulin exocytosis. J Cell Mol Med 21: 2950-2962, 2017.
4. Bogan JS, Xu Y and Hao M: Cholesterol accumulation increases insulin granule size and impairs membrane trafficking. Traffic 13: 1466-1480, 2012.
5. Kruit JK, Kremer PH, Dai L, Tang R, Ruddle P, de Haan W, Brunham LR, Verchere CB and Hayden MR: Cholesterol efflux via ATP-binding cassette transporter A1 (ABCA1) and cholesterol uptake via the LDL receptor influences cholesterol-induced impairment of beta cell function in mice. Diabetologia 53: 1110-1119, 2010.
6. Poy MN, Eliasson L, Krutzfeldt J, Kuwajima S, Ma X, Macdonald PE, Pfeffer S, Tuschl T, Rajewsky N, Rorsman P and Stoffel M: A pancreatic islet-specific microRNA regulates insulin secretion. Nature 432: 226-230, 2004.
7. Osmai M, Osmai Y, Bang-Berthelsen CH, Pallesen EM, Vestergaard AL, Novotny GW, Pociot F and Mandrup-Poulsen T: MicroRNAs as regulators of beta-cell function and dysfunction. Diabetes Metab Res Rev 32: 334-349, 2016.
8. Li Y, Luo T, Wang L, Wu J and Guo S: MicroRNA-19a-3p enhances the proliferation and insulin secretion, while it inhibits the apoptosis of pancreatic cells via the inhibition of SOCS3. Int J Mol Med 38: 1515-1524, 2016.
9. Tugay K, Guay C, Marques AC, Allagnat F, Locke JM, Harries LW, Rutter GA and Regazzi R: Role of microRNAs in the age-associated decline of pancreatic beta cell function in rat islets. Diabetologia 59: 161-169, 2016.
10. Zhu Y, You W, Wang H, Li Y, Qiao N, Shi Y, Zhang C, Bleich D and Han X: MicroRNA-24/MODY gene regulatory pathway mediates pancreatic beta-cell dysfunction. Diabetes 62: 3194-3206, 2013.

11. Malenczyk K, Girach F, Szodorai E, Storm P, Segerstolpe A, Tortoriello G, Schnell R, Mulder J, Romanov RA, Borok E, *et al*: A TRPV1-to-secretagogin regulatory axis controls pancreatic beta-cell survival by modulating protein turnover. EMBO J 36: 2107-2125, 2017.
12. Wagner L, Oliyarnyk O, Gartner W, Nowotny P, Groeger M, Kaserer K, Waldhausl W and Pasternack MS: Cloning and expression of secretagogin, a novel neuroendocrine- and pancreatic islet of langerhans-specific Ca2+-binding protein. J Biol Chem 275: 24740-24751, 2000.
13. Yang SY, Lee JJ, Lee JH, Lee K, Oh SH, Lim YM, Lee MS and Lee KJ: Secretagogin affects insulin secretion in pancreatic beta-cells by regulating actin dynamics and focal adhesion. Biochem J 473: 1791-1803, 2016.
14. Livak KJ and Schmittgen TD: Analysis of relative gene expression data using real-time quantitative PCR and the 2(-Delta Delta C(T)) method. Methods 25: 402-408, 2001.
15. Lv YC, Tang YY, Peng J, Zhao GJ, Yang J, Yao F, Ouyang XP, He PP, Xie W, Tan YL, *et al*: MicroRNA-19b promotes macrophage cholesterol accumulation and aortic atherosclerosis by targeting ATP-binding cassette transporter A1. Atherosclerosis 236: 215-226, 2014.
16. Staaf J, Ubhayasekera SJ, Sargsyan E, Chowdhury A, Kristinsson H, Manell H, Bergquist J, Forslund A and Bergsten P: Initial hyperinsulinemia and subsequent beta-cell dysfunction is associated with elevated palmitate levels. Pediatr Res 80: 267-274, 2016.
17. Barlow J, Jensen VH, Jastroch M and Affourtit C: Palmitate-induced impairment of glucose-stimulated insulin secretion precedes mitochondrial dysfunction in mouse pancreatic islets. Biochem J 473: 487-496, 2016.
18. Tiwari J, Gupta G, de Jesus Andreoli Pinto T, Sharma R, Pabreja K, Matta Y, Arora N, Mishra A, Sharma R and Dua K: Role of microRNAs (miRNAs) in the pathophysiology of diabetes mellitus. Panminerva Med 60: 25-28, 2018.
19. Hashimoto N and Tanaka T: Role of miRNAs in the pathogenesis and susceptibility of diabetes mellitus. J Hum Genet 62: 141-150, 2017.
20. Calderari S, Diawara MR, Garaud A and Gauguier D: Biological roles of microRNAs in the control of insulin secretion and action. Physiol Genomics 49: 1-10, 2017.
21. Gu C, Stein GH, Pan N, Goebbels S, Hornberg H, Nave KA, Herrera P, White P, Kaestner KH, Sussel L and Lee JE: Pancreatic beta cells require NeuroD to achieve and maintain functional maturity. Cell Metab 11: 298-310, 2010.
22. Zhang ZW, Zhang LQ, Ding L, Wang F, Sun YJ, An Y, Zhao Y, Li YH and Teng CB: MicroRNA-19b downregulates insulin 1 through targeting transcription factor neuroD1. FEBS Lett 585: 2592-2598, 2011.
23. Lee JJ, Yang SY, Park J, Ferrell JE Jr., Shin DH and Lee KJ: Calcium ion induced structural changes promote dimerization of secretagogin, which is required for its insulin secretory function. Sci Rep 7: 6976, 2017.
24. Kobayashi M, Yamato E, Tanabe K, Tashiro F, Miyazaki S and Miyazaki J: Functional analysis of novel candidate regulators of insulin secretion in the MIN6 mouse pancreatic beta cell line. PLoS One 11: e0151927, 2016.
25. Bazwinsky-Wutschke I, Wolgast S, Muhlbauer E and Peschke E: Distribution patterns of calcium-binding proteins in pancreatic tissue of non-diabetic as well as type 2 diabetic rats and in rat insulinoma beta-cells (INS-1). Histochem Cell Biol 134: 115-127, 2010.
26. Segerstolpe A, Palasantza A, Eliasson P, Andersson EM, Andreasson AC, Sun X, Picelli S, Sabirsh A, Clausen M, Bjursell MK, *et al*: Single-cell transcriptome profiling of human pancreatic islets in health and Type 2 diabetes. Cell Metabo 24: 593-607, 2016.
27. Hansson SF, Zhou AX, Vachet P, Eriksson JW, Pereira MJ, Skrtic S, Jongsm Wallin H, Ericsson-Dahistrand A, Karlsson D, Ahnmark A, *et al*: Secretagogin is increased in plasma from type 2 diabetes patients and potentially reflects stress and islet dysfunction. PLoS One 13: e0196601, 2018.
28. Rorsman P and Renstrom E: Insulin granule dynamics in pancreatic beta cells. Diabetologia 46: 1029-1045, 2003.
29. Heaslip AT, Nelson SR, Lombardo AT, Beck Previs S, Armstrong J and Warshaw DM: Cytoskeletal dependence of insulin granule movement dynamics in INS-1 beta-cells in response to glucose. PLoS One 9: e109082, 2014.
30. Rondas D, Tomas A and Halban PA: Focal adhesion remodeling is crucial for glucose-stimulated insulin secretion and involves activation of focal adhesion kinase and paxillin. Diabetes 60: 1146-1157, 2011.